IOPscience iopscience.iop.org

Home Search Collections Journals About Contact us My IOPscience

Ion-beam-induced enhanced diffusion from gold thin films in silicon

This article has been downloaded from IOPscience. Please scroll down to see the full text article.

2008 J. Phys.: Condens. Matter 20 485008

(http://iopscience.iop.org/0953-8984/20/48/485008)

View the table of contents for this issue, or go to the journal homepage for more

Download details:
IP Address: 129.252.86.83
The article was downloaded on 29/05/2010 at 16:41

Please note that terms and conditions apply.

IOP PUBLISHING JOURNAL OF PHYSICS: CONDENSED MATTER

J. Phys.: Condens. Matter **20** (2008) 485008 (5pp) doi:10.1088/0953-8984/20/48/485008

Ion-beam-induced enhanced diffusion from gold thin films in silicon

J Ghatak[1], B Sundaravel[2], K G M Nair[2] and P V Satyam[1]

[1] Institute of Physics, Bhubaneswar 751005, India
[2] Materials Science Division, Indira Gandhi Center for Atomic Research, Kalpakkam 603102, India

E-mail: satyam@iopb.res.in

Received 15 July 2008, in final form 9 September 2008
Published 6 November 2008
Online at stacks.iop.org/JPhysCM/20/485008

Abstract
We report enhanced diffusion of gold atoms from gold films of various thicknesses (that are deposited on Si) due to 1.5 MeV Au^{2+} ion impacts under high flux conditions. The maximum depths of mass transport have been found to be 95, 160 and 13 nm for the cases of 5.3, 10.9 and 27.5 nm thick gold films, respectively, at a fluence of 1×10^{14} ions cm^{-2}. Interestingly, at a higher fluence of 1×10^{15} ions cm^{-2}, gold atoms from the 27.5 thick films are transported to a maximum depth of 265 nm in the substrate. The enhanced diffusion for various film thicknesses is consistent with the recoil profiles of Au atoms into Si, which are obtained using Monte Carlo simulations (TRIM). These results have been explained on the basis of the ion-beam-induced flux-dependent amorphous nature of the substrate, and transient beam-induced temperature effects. This work also confirms the absence of ion-induced spike confinement effects that might arise from the morphological nature of the isolated nanostructures.

(Some figures in this article are in colour only in the electronic version)

1. Introduction

The study of the diffusion of noble metals in crystalline silicon has been actively pursued due to various technological applications and associated fundamental issues. As the size of electronic devices is shrinking to the nanometer regime, a better understanding of the effect of material interfaces at the atomic scale is necessary. Gold is widely used in electronic devices to control the base minority-carrier lifetime due to its ability to act as a recombination center when dissolved in silicon [1]. In the fabrication of such devices, gold is introduced into silicon wafers by a high temperature diffusion process following vacuum evaporation of metallic gold onto the surfaces. It is also well known that gold thin films act as contact layers in many systems for electronic measurements. Hence, the diffusion of gold atoms in crystalline silicon plays an important role. Two mechanisms, namely the 'Frank–Turnbull' mechanism [2] and the 'kick-out' mechanism [3], have been used to explain the gold atoms' diffusion in crystalline silicon. In the case of amorphous silicon, the Au diffusion was explained in terms of direct diffusion, wherein the diffusing Au atoms were temporarily trapped by different kinds of vacancy-like effects [4, 5]. In general, at high enough temperatures, the amorphous silicon (a-Si) recrystallizes and hence it would be difficult to study the diffusion of gold atoms in an a-Si system. Past investigations on Au-implanted silicon systems suggested about the gold segregation as a result of gold atoms being expelled from the recrystallized amorphous layer during thermal and ion beam annealing [6, 7]. Also, it was reported that the Au solid solubility [8] and diffusivity [9, 10] in crystalline silicon (c-Si) is *lower* than that in amorphous silicon (a-Si). In the study of precipitation of implanted atoms, both the segregation and diffusion of gold atoms has been found to play a role. When the implanted Au concentration exceeded the local solubility, Au precipitates were expelled from the matrix, resulting in segregation into dense defect regions [11].

Interesting differences for *ion–uniform film* and *ion–nanostructure film* interaction phenomena relating to ion beam mixing and surface morphological effects were reported [12–14]. It was found that ion-beam-induced mixing was present in the nanostructured Au/Si systems and was found to be absent for thick and continuous Au/Si systems under low flux irradiation conditions (≈10^{10} ions cm^{-2} s^{-1}) [13]. Dramatic mass transport has been observed from Au *nanostructures* into the Si at high flux irradiation conditions

 © 2008 IOP Publishing Ltd Printed in the UK

(6.3×10^{12} ions cm^{-2} s^{-1}). In this case, the mass transport was found to extend up to a distance of about 60 nm into the substrate, much beyond the size of the nanostructures themselves [14]. In the present work, we report enhanced mass transport from various thicknesses of gold films deposited on silicon under high flux irradiation conditions. The surface morphology of the gold films varied for different thicknesses. In as-deposited systems, for low thickness films (for <5.3 nm thick gold films) isolated gold nanostructures were observed while for larger thickness films (10.9 and 27.5 nm thick films) uniform and continuous layers were observed. In our previous work using low flux irradiation experiments, while explaining the enhanced crater formation from nanostructures, we had proposed the possibility of an ion-induced energy spike in the nanostructures that is arising due to the spatially confined nature of these structures [12]. In this paper, we confirmed that the mass transport was not because of direct cascade-induced flow and no evidence was found for confinement effects. We present a plausible mechanism to understand the enhanced diffusion phenomenon for various thicknesses of Au films on silicon.

2. Experimental methods

Au films of thicknesses ≈5.3, 10.9 and 27.5 nm were deposited at room temperature by thermal evaporation using a resistive heating method in high vacuum conditions (≈4×10^{-6} mbar). A ≈2 nm thick native oxide was present on Si(111) substrates. The substrates were cleaned with de-ionized water followed by rinsing in methanol and acetone prior to deposition. For 5.3 nm samples, the deposition rate was kept at ≈0.01 nm s^{-1}. The deposition rate was kept at ≈0.1 nm s^{-1} for 10.9 and 27.5 nm samples. The thickness of each Au film was determined using Rutherford backscattering spectrometry (RBS) measurements and using simulations [15]. During the simulations, the density of bulk Au was used to obtain the thickness values. All the irradiations were carried out with 1.5 MeV Au^{2+} ions and with an ion flux 6.3×10^{12} ions cm^{-2} s^{-1} (corresponding to a current density of 2.0 μA cm^{-2}) using the 1.7 MV Tendetron accelerator. During the irradiation, the substrates were kept at room temperature. The fluences on the samples were varied from 1×10^{14} to 1×10^{15} ions cm^{-2}. The substrates were oriented 5° off normal to the incident beam to suppress the channeling effects. The RBS measurements were carried out with 1.35 MeV He^{+} ions. Cross-sectional transmission electron microscopy (XTEM) measurements were performed using a JEOL JEM-2010 operating at 200 kV on the irradiated samples to study the surface and interface modifications. XTEM samples were prepared by mechanical thinning followed by 3.5 keV Ar ion milling. It is important to note that the projected ranges (determined using TRIM simulation) of 1.5 MeV Au ions in Au and Si are ≈96 and 320 nm, respectively [16]. This implies that the impinging gold ions would penetrate deep into the Si substrate, much more than the average height of the Au layers for all cases. The maximum depth for diffused gold atoms in silicon was found to be 265 nm (table 1). Hence the mass transport that was observed is not from the impinging ions.

Table 1. Depths to which gold atoms are diffused for various film thicknesses as a function of flux and fluence are given.

Film thickness (nm)	Fluence (ions cm^{-2})	Depth at low flux (nm)	Depth at high flux (nm)
2.0	6×10^{13}	Nil [14]	60 [14]
5.3	1×10^{14}	Nil [13]	95.0
10.9	1×10^{14}	Nil [13]	160.0
27.5	1×10^{14}	Nil [13]	13.0
27.5	1×10^{15}	—	265.0

3. Experimental results

A direct observation of dramatic mass transport due to 1.5 MeV Au^{2+} ion impact has been observed for lower thickness films (≈2.0 nm Au on Si) when the irradiations were carried out under high flux (3.2×10^{10} to 6.3×10^{12} ions cm^{-2} s^{-1}) conditions. The nanostructures were formed as a result of the non-wetting nature of Au on the oxide layer. The average size and height of these nanostructures were found to be 7.6 and 6.9 nm, respectively. In these results, the maximum mass transport into the substrate was found to extend up to a distance of about 60 nm, much beyond the size of the nanostructures present on the surface [14].

Figures in 1(a) and (b) are the bright-field (BF) XTEM images corresponding to as-deposited films of thicknesses 5.3 and 10.9 nm, respectively. The effective thickness values of 5.3 and 10.9 nm were determined using RBS, but the XTEM measurements showed the thickness to be 15.0 and 17.5 nm. For the pristine film of thickness 5.3 nm, XTEM images show large isolated nanostructures. This shows the non-uniformity nature of the films. For the film thickness of 10.9 nm, the uniformity and the coverage area of gold nanostructures increases. The irradiation effects at a fluence of 1×10^{14} ions cm^{-2} with flux 6.3×10^{12} ions cm^{-2} s^{-1} are shown in figures 1(c) and (d) for 5.3 and 10.9 nm gold on Si(111) samples, respectively. For these two cases, enhanced diffusion was observed from the top gold layer into the Si substrate. In the case of the 5.3 nm Au/Si system, the maximum depth for Au atoms diffused into the Si substrates has been found to be ≈95 nm, while, the maximum transported depth of 160 nm was found for the 10.9 nm Au/Si system (figure 1(d)). This implies more mass transport for the 10.9 nm thick Au case compared to both the 2.0 and 5.3 nm thick gold film cases. The contrast in the bright-field images (figures 1(c) and (d)) was attributed to the contribution from the diffused gold atoms (i.e. presence of gold atoms at larger depth in the interfacial region). These observations reveal that the amount of mass transport (and maximum depth) increases with the increase in top Au layer thickness, ruling out any confinement effects that would possibly be there due to the isolated nature of the nanostructures. Figure 1(e) corresponds to the selected-area electron diffraction (SAED) pattern taken from the implanted region (circular region of figure 1(d)) of 10.9 nm Au. The SAED pattern confirms the amorphization nature of the Si substrate at this fluence. Similarly, the Si substrate was found to be amorphized for the case of a 5.3 nm thick Au film also. Hence, the diffusion that was observed

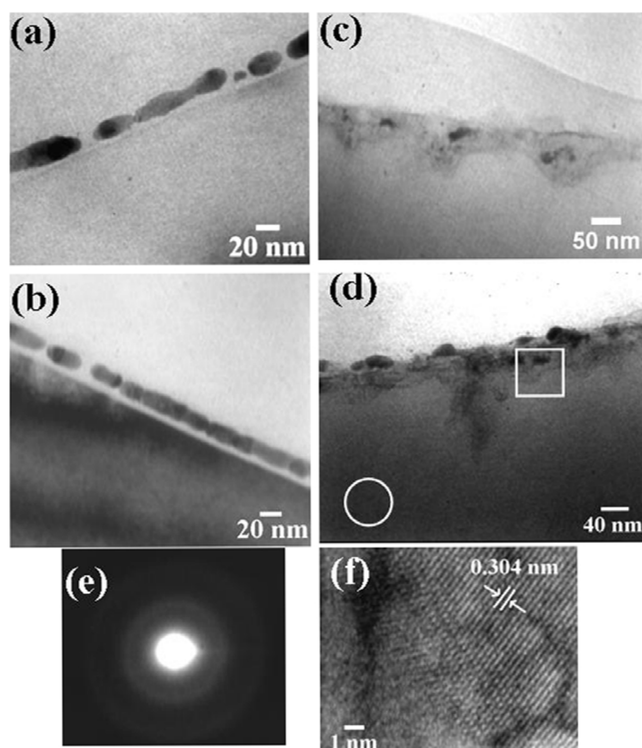

Figure 1. Cross-sectional bright-field TEM (XTEM) micrographs for pristine Au/Si systems: (a) 5.3 nm and (b) 10.9 nm Au/Si system. (c) and (d) correspond to the irradiated systems corresponding to 5.3 and 10.9 nm Au/Si systems, respectively. (e) The SAED pattern shows the amorphous nature of the implanted region of the substrate. (f) The high resolution cross-sectional bright-field TEM image of the rectangular region of figure (d).

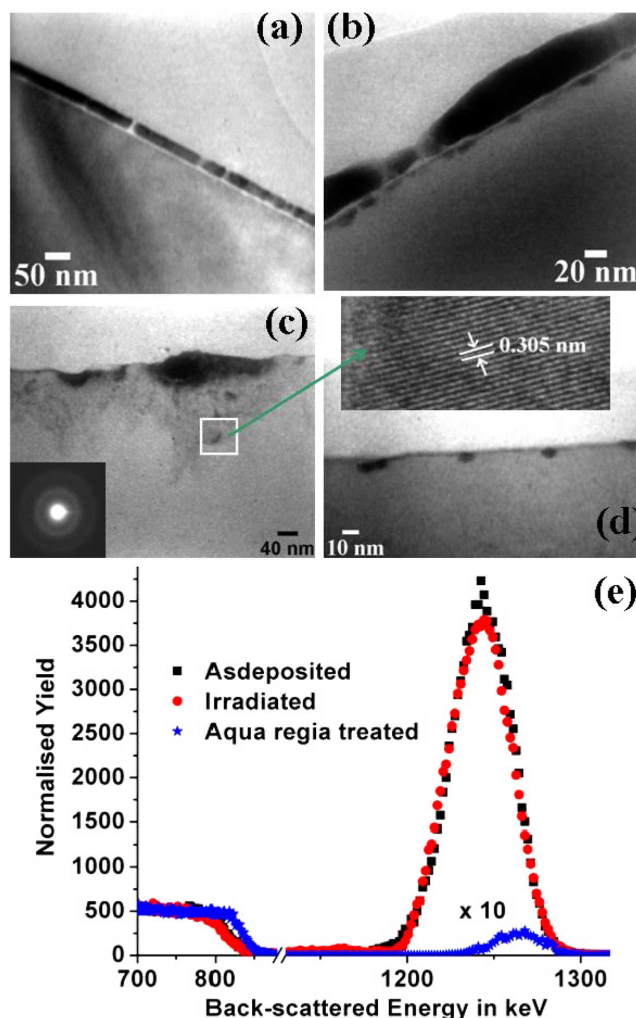

Figure 2. (a) The XTEM micrograph of pristine 27.5 nm Au/Si. (b) and (c) are the XTEM micrographs of 27.5 nm Au/Si after irradiation at a fluence of 1×10^{14} and 1×10^{15} ions cm^{-2}, respectively. Inset of figure (c) depicts the SAED pattern after irradiation from the implanted region of the Si substrate. The high resolution XTEM image was taken from the rectangular region of figure (f) which is shown by the arrow mark. (d) The XTEM micrograph of an aqua regia etched irradiated sample while the fluence was 1×10^{14} ions cm^{-2}. (e) The RBS spectra of irradiated 27.5 nm Au/Si systems before and after aqua regia treatment.

in these cases was attributed to the amorphous nature of the silicon substrate. It is interesting to note the crystalline phase was formed in the mixed layer. Figure 1(f) is taken from the rectangular region (near the surface) of figure 1(d) (for the irradiated 10.9 nm Au/Si system). The selected region is crystalline in nature with the lattice spacing corresponding to 0.304 ± 0.005 nm, indicating a possible formation of an Au_5Si_2 phase. This phase formation indicates that the mass transport is associated with the thermal reaction. More details about the silicide formation have been reported elsewhere [14, 17].

The role of the crystalline nature of the substrate for the enhanced diffusion of gold atoms is evident from the mass transport studies in the 27.5 nm thick film case. Figure 2(a) depicts the bright-field XTEM micrographs for the pristine Au film thickness of 27.5 nm. The TEM measurements show that the morphology of the Au film was uniform in nature, unlike the thinner film cases (5.3 and 10.9 nm thick). Figures 2(b) and (c) show the XTEM micrographs of the irradiated 27.5 nm Au/Si system at the flux 6.3×10^{12} ions cm^{-2} s^{-1} and at fluence values of 1×10^{14} and 1×10^{15} ions cm^{-2}, respectively. Interestingly, for the case of the 27.5 nm Au/Si system, a maximum depth of only $\approx$13 nm was observed at a fluence of 1×10^{14} ions cm^{-2} (figure 2(b)). It is to be noted that, at this fluence (1×10^{14} ions cm^{-2}) and flux (6.3×10^{12} ions cm^{-2} s^{-1}), large mass transport was observed for thinner film cases (5.3 and 10.9 nm thick Au/Si systems). The mass transport was found to increase dramatically up to a depth of 265 nm for the thick film case at fluence 1×10^{15} ions cm^{-2} (figure 2(c)). The inset of figure 2(c) shows the SAED pattern from the implanted region of the substrate, which indicates the amorphous nature. The high resolution lattice image taken from the rectangular region of figure 2(c) shows the formation of an Au–Si alloy as mentioned earlier (similar to figure 1(f)). We conclude that high flux MeV ion irradiation leads to alloy formation for various thicknesses of Au films.

XTEM and RBS measurements on an aqua regia (HNO_3: HCL = 1:3) treated irradiated sample (27.5 nm thick Au film irradiated at the fluence 1×10^{14} ions cm^{-2}) were carried out to check the presence of reacted gold on the surface and diffusion into the substrate. It is known that un-reacted gold would be etched by aqua regia. Figure 2(d) shows the BF XTEM of the

aqua regia treated sample, confirming the absence of gold on the surface (either un-reacted or reacted gold were not present). Figure 2(e) depicts the RBS spectra for pristine, irradiated and aqua regia etched conditions. For the sake of visualization, only the Au signal for the aqua regia treated sample has been magnified (multiplied by a factor of 10). RBS measurements confirm the presence of gold (in the silicon substrate) even after aqua regia treatment, showing the embedded nature of the gold film. The shift of the Si edge to a higher energy and the shift of the Au edge to a lower energy confirm the presence of Au embedded in the Si, rather than the presence of an Au layer on the Si surface. This is in agreement with XTEM measurements.

From the results for various thicknesses of Au films, it is clear that the distributed depth of Au atoms is not equal for all systems. The quantitative analysis for all the systems at different flux and fluence values is given in table 1. From these results, it is clear that enhanced diffusion has been observed for higher thickness films and high enough fluence values. We discuss plausible mechanisms to explain these interesting results.

XTEM measurements in the case of the 5.3 and 10.9 nm Au/Si systems show the average film thickness to be about 15.0 and 17.5 nm, respectively (from XTEM measurements). The nuclear energy loss and the electronic energy loss for 1.5 MeV Au ions in Au are 9.5 and 2.5 keV nm^{-1}, respectively [16]. Therefore, the total energy loss in the 15.0 nm Au target (i.e. 5.3 nm Au/Si systems) due to 1.5 MeV Au ions is 180 keV which comes out to be less than the energy required for the Au atoms to reach a depth of 95 nm inside Si. To reach a depth of 95 nm, the required energy for the gold recoiled atoms should be ≈300 keV [16]. Hence, the TRIM simulation results cannot explain the enhanced diffusion. The mass transportation to a depth of 13 nm for high flux and low fluence (1×10^{14} ions cm^{-2}) can be considered as recoiled or ballistically mixed events. From the present and earlier experimental results [14], it is clear that the recoil of Au atoms from the top Au layer was highly influenced by the ion beam flux and the nature of the substrate (in terms of defect concentration).

The incident beam flux can affect the diffusion process due to the significant changes that occur in amorphization and effective wafer temperature of the silicon substrate. It is known that, in semiconductors, defect concentration increases with the increase in ion flux and results in a faster amorphization process (at lower fluence with higher flux) [18]. That means at a given temperature, with higher flux, a lower fluence is needed to achieve amorphization whereas with a lower flux, the defect concentration has to be compensated by a higher fluence [19]. From the previous flux-dependent study, the amorphization has been observed at fluence 6×10^{13} ions cm^{-2} with ion flux 6.3×10^{12} ions cm^{-2} s^{-1} [14]. This value is smaller compared to the earlier observations [20] and hence we may infer that the higher flux leads to faster amorphization. This appears to be realistic as the displacement production (vacancy–interstitial pair) rate is proportional to the incident ion flux [21]. We have estimated the wafer temperature during irradiation [14] using the experimentally verified prescription given by Nakata [22].

One can divide the diffusion into two regimes: temperature-dependent (thermal diffusion) and temperature-independent (radiation-enhanced diffusion). In the temperature-dependent regime, thermal diffusivity is proportional to the substrate temperature. There is a critical temperature (T_c) that exists, above which the radiation-enhanced diffusion (RED) is found to be significant [23]. It is to be noted that $T_c = 422$ K for the Au–Si case [24], which is less than the wafer temperature during irradiation due to beam heating. Under the present high flux and high fluence irradiation conditions, the temperature of the wafer is high enough for diffusion to dominate in a partially amorphous system (note that the diffusivity of Au in a-Si is more than that of c-Si [9, 10]). This is due to the excess displacements created at higher beam flux irradiation conditions. These guide the recoiled Au atoms and possibly migrate in the substrate as substitutional (kick-out mechanism) atoms [3]. Hence during irradiation, as soon as the amorphization takes place in the Si substrate, the diffusivity of recoiled Au atoms increases drastically. An estimate can be made for the transported distances from the marker layer model due to ballistic cascade mixing [25]. Considering the values of diffusivity $D_{cas} \approx 700$ nm^2 s^{-1} at $T \approx 1000$ K [9] and average deposited energy $F_D(x) = 1761$ eV nm^{-1} [16], the transported depth under these conditions would be ≈250 nm, which matches well fairly with our observed transported depth and justifies the consideration of diffusion phenomena associated with the mass transport.

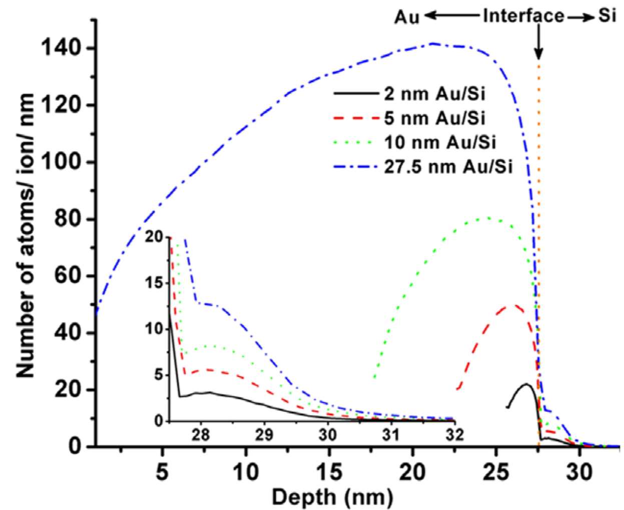

Figure 3. TRIM profile for Au recoiled atom distribution due to 1.5 MeV Au ions. The Au thicknesses used in the simulation are 2, 5, 10 and 27.5 nm. The inset corresponds to the zoomed recoil distribution of Au only into the Si for all the above-mentioned Au films.

The difference in transported depth for various film thicknesses will be discussed in the following section. For example, in the case of 5.3 nm Au/Si, the maximum depth of distributed Au is about 95 nm, whereas it is 265 nm for 27.5 nm Au/Si. In figure 3, the Au recoil distributions of 2.0, 5.0, 10.0 and 27.5 nm systems due to 1.5 MeV Au at normal incidence obtained using the TRIM simulation have been plotted [16]. In the inset of figure 3, the zoomed recoil distribution of Au atoms into the Si for all the above-mentioned Au film thicknesses has been shown. It is clear from the figure that the amount of recoiled gold atoms into Si (i.e. number

of recoiled Au atoms per unit length (depth) of Si) is greater for higher film thickness. So, if the available number of recoiled gold atoms is more at the interface, then the area of the redistributed region will be larger and hence the transported depth will also be larger. Also one needs to consider the role of the amorphization. For the same energetic ion beam, there will be different onset fluence values for complete amorphization of Si substrates with different thicknesses of Au films. This is due to the fact that, in Si with thicker films, nuclear energy loss inside the film will be more and hence needs a higher fluence for complete amorphization of the Si substrate. Hence there will be definite differences in defect concentration for various thicknesses of films at the same fluence. It was clearly shown that Au diffusion from the top Au layer is more in a-Si than in c-Si and any intermediate crystalline layer (that is partially a-Si) will suppress the effect [5]. Hence, the depth of the mass transport or diffusion region is more at a fluence 1×10^{15} ions cm^{-2} than that at 1×10^{14} ions cm^{-2} in the case of 27.5 nm Au/Si systems. We therefore propose the following mechanism to understand the enhanced diffusion of gold in silicon: (i) collision cascades drive gold atoms from the film into the substrate through ballistic mixing and recoil implantation processes, (ii) this is followed by amorphization in the substrate that occurs at lower fluence at high flux conditions, (iii) the effective wafer temperature due to incident beam power drives the mass transport (enhanced diffusion occurring for gold atoms in an a-Si system).

4. Conclusions

Enhanced mass transport for various thicknesses of Au films starting from nanoislands (5.3 nm Au/Si) to a thick continuous film (27.5 nm Au/Si) due to MeV Au ion bombardment under high flux irradiation conditions has been presented. The transported depth is found to be more for larger thicknesses of the gold overlayer. The amount of recoiled Au atoms from the top Au layer is found to be more for larger thickness Au film and are consistent with the TRIM simulation. Mass transport in all the samples suggests that the thermal spike confinement is not significant. High flux causes faster amorphization and the rise in wafer temperature helps in faster diffusion of the recoiled Au atoms.

References

[1] Bullis W M 1966 *Solid-State Electron.* **9** 143

[2] Frank F C and Turnbull D 1956 *Phys. Rev.* **104** 617

[3] Gösele U, Frank W and Seeger A 1980 *Appl. Phys.* **23** 36

[4] Coffa S, Poate J M, Jacobson D C, Frank W and Gustin W 1992 *Phys. Rev.* B **45** 8355
Frank W 1997 *Defect Diffus. Forum* **143–147** 695
Frank W, Gustin W and Horz M 1996 *J. Non-Cryst. Solids* **205–207** 208

[5] Ehrhardt J, Klimmer A, Eisenmenger J, Muller T, Boyen H G, Ziemann P, Biskupek J and Kaiser U 2006 *J. Appl. Phys.* **100** 063534

[6] Poate J M, Priolo F, Jacobson D C, Batstone J L and Thompson M O 1989 *Nucl. Instrum. Methods* B **37/38** 955

[7] Jacobson D C, Poate J M and Olson G L 1986 *Appl. Phys. Lett.* **43** 118

[8] Lindner J K N, Heckling N and te Kaat E 1987 *Nucl. Instrum. Methods* B **26** 551

[9] Poate J M, Jacobson D C, Williams J S, Elliman R G and Boerma D O 1987 *Nucl. Instrum. Methods Phys. Res.* B **19/20** 480

[10] Priolo F, Poate J M, Jacobson D C, Linnros J, Batstone J L and Campisano S U 1988 *Appl. Phys. Lett.* **52** 1213

[11] Alford T L and Theodore N D 1994 *J. Appl. Phys.* **76** 7265

[12] Satyam P V, Kamila J, Mohapatra S, Satpati B, Goswami D K, Dev B N, Cook R E, Assoufid L, Wang J and Mishra N C 2003 *J. Appl. Phys.* **93** 6399

[13] Satpati B, Satyam P V, Som T and Dev B N 2004 *Appl. Phys.* A **79** 447
Satpati B, Satyam P V, Som T and Dev B N 2004 *J. Appl. Phys.* **96** 5212

[14] Ghatak J, Bhatta U M, Sundaravel B, Nair K G M, Liou S-C, Chen C-H, Wang Y-L and Satyam P V 2008 *Nanotechnology* **19** 325602

[15] Mayer M 1999 *Proc. 15th Int. Conf. on the Application of Accelerators in Research and Industry* vol 467 (*American Institute of Physics Conference Proceedings*) ed J L Duggan and I L Morgan (New York: AIP) p 541

[16] Biersack J P and Haggmark L 1980 *Nucl. Instrum. Methods* **174** 257 (also see www.srim.org)

[17] Tsaur B Y and Mayer J W 1981 *Phil. Mag.* A **43** 345

[18] Haynes T E and Holland O W 1991 *Appl. Phys. Lett.* **59** 452

[19] Goldberg R D, Elliman R G and Williams J S 1995 *Nucl. Instrum. Methods Phys. Res.* B **106** 242

[20] Kamila J, Satpati B, Goswami D K, Rundhe M, Dev B N and Satyam P V 2003 *Nucl. Instrum. Methods Phys. Res.* B **207** 291

[21] Sigmund P 1969 *Appl. Phys. Lett.* **14** 169

[22] Nakata J 1991 *Phys. Rev.* B **43** 14643

[23] Matteson S 1979 *Radiat. Eff.* **42** 217

[24] Cheng Y T, Zhao X A, Banwell T, Workman T W, Nicolet M A and Johnson W L 1986 *J. Appl. Phys.* **60** 2615

[25] Sigmund P and Gras-Marti A 1981 *Nucl. Instrum. Methods* **182/183** 25